IJME

Int. J. of Applied Mechanics and Engineering, 2026, vol.31, No.1, pp.108-122
DOI: 10.59441/ijame/214146

STRENGTHENING OF REINFORCED NORMAL AND SELF-COMPACTED CONCRETE BEAMS: COMPARATIVE EXPERIMENTAL INVESTIGATION

R.O. Mustafa[1], B.R. Hassan[2], M.A. Abdulrehman[3*], H.A. Goaiz[4] and A.Q. Moften[3]
[1]Civil Engineering Department, University of Sulaimani, IRAQ
[2]Civil Engineering Department, University of Halabja, Halabja, IRAQ
[3]Materials Engineering, Mustansiriyah University, IRAQ
[4]Civil Engineering Department, University of Wasit, IRAQ
E-mail: mohammed_ali_mat@uomustansiriyah.edu.iq

Carbon fiber reinforced polymer (CFRP) is a sustainable and long-lasting material that can improve concrete strength in many different structural contexts. This work shows how well near-surface mounted (NSM) CFRP improves the flexural behavior of both self-compacted and normal-strength reinforced concrete beams. Six sets of reinforced concrete beams were cast in three groups with normal-strength concrete and three groups with self-compacted concrete. Four groups were externally strengthened using NSM-CFRP bars, and the remaining two groups acted as control beams without CFRP reinforcement. Two NSM groups had CFRP bars placed at the sides of the beams, whereas in the other NSM two groups, the bars were buried at the bottom. For normal-strength concrete and self-compacted concrete, the experimental findings showed that side-mounted NSM-CFRP bars increased the flexural strength by *32%* and *44%*, respectively. The flexural strength increases were *25%* and *38%* when mounted at the bottom. The novelty of this work lies in its comparative evaluation of two CFRP installation procedures across two concrete types under consistent structural and testing conditions, a feature not thoroughly investigated in previous work. This dual-variable approach provides a useful understanding of how to maximize CFRP retrofitting strategies depending on the concrete type and application situation.

Key words: carbon fibre polymer bar, flexure, near surface mounted NSM, strengthening.

1. Introduction

Concrete is an indispensable and practical material used in construction projects [1]. The strength and quality of concrete are highly dependent on the mixing proportions of the binding material, coarse and fine aggregates, admixture, and water [2]. Concrete is reliable, inexpensive, easily shaped into various forms and sizes, and can be set quickly. Its purpose is to facilitate dependable and superior fast-track building [3]. Construction projects built using concrete members should take measurements to be strong enough to withstand typhoons, hurricanes, tornadoes, and earthquakes [4]. Despite all the advancements in science, there still needs to be a way from the harm that nature causes. Concrete industry experts are looking for ways to improve the economics and performance of concrete to reduce its environmental impact. Experts are taking notice of replacing or reducing one of the mix compositions with new materials, such as waste plastic, glass, pozzolanic materials [5-9] or developing new concrete materials and mixtures such as foam concrete, pervious concrete, self-compact concrete, and reactive powder concrete [10-13]. These improvements were made to the material quality. While concrete is used in structural members, several studies have been conducted to check the state and improve the properties of members, as it is composed of concrete and reinforcement [14]. The members' behaviors were enhanced owing to the use of different types of concrete with different reinforcement designs or reinforcement types.

Self-compacting concrete (SCC) is a type of concrete that can flow and compact without external forces or vibrations. The advent of SCC has resulted in a significant breakthrough in concrete technology in

* To whom correspondence should be addressed

recent times. SCC is a type of concrete that can flow easily through formwork, around reinforcements, and into tight spaces without the need for additional vibration, and with the ability to set under its weight without segregation or bleeding easily. Viscosity-adjusting additives can also be used to increase the viscosity of a paste [15]. Normal-strength concrete (NSC) is a globally prevalent construction material. It is a composite material composed of a blend of cement, aggregates, and water, which hardens over time to form a solid structure. NSC has a compressive strength of approximately *20-40 MPa*, making it appropriate for various construction applications [16].

This improvement may be due to the use of a new type of reinforcement instead of steel bars, such as carbon fiber-reinforced polymers (CFRP). Recently, CFRP bars have become increasingly popular substitutes for conventional steel reinforcements. CFRP bars comprise carbon fibers and a polymer matrix, typically epoxy resin. This reinforcement material offers several advantages over steel reinforcement, including a high strength-to-weight ratio, resistance to corrosion, and exceptional resistance to fatigue [17]. CFRP bars are used in various applications including civil engineering and construction. They are particularly useful for structures subjected to severe conditions, such as bridges, buildings, and tunnels. CFRP bars have also been used in seismic retrofitting to improve the seismic performance of existing structures. The high strength and stiffness of CFRP bars can help improve the structural integrity of buildings, making them more resistant to earthquakes and other seismic events [18].

Many researchers have used CFRP in beams using NSM, which is a method of strengthening and retrofitting concrete structures using FRP composites. This approach has garnered substantial interest in recent years owing to its effectiveness and practicality in enhancing the performance of existing structures [19]. El-Wakkad [20], examined multiple traditional techniques along with a novel shear reinforcement approach for reinforced self-compacting concrete (RSCC) deep beams. A total of 16 RSCC deep beams were reinforced using different materials, such as steel, glass, and carbon fiber-reinforced polymers (GFRP and CFRP), which were used in an experimental test program. Near-surface-mounted reinforcement (NSMR) and externally bonded layers (EBL) have been employed as two distinct approaches. The outcomes of the novel method, which uses roving NSM GFRP rods wet with epoxy, were compared with those of alternative methods. The load capacity of the GFRP rod anchoring increased by *36%* to *55%* using the new shear strengthening method, depending on the length. De-Lorenzis *et al.* [21], conducted an analysis on the tensile characteristics of Fibre Reinforced Polymer (FRP) materials. When no manufacturer's data were available and coupon-sized samples were used to study the bonding behavior of NSM-FRM bars incorporated within concrete or masonry units, they examined the structural performance of reinforced concrete (RC) beams subjected to shear forces by utilizing full-scale specimens reinforced with NSM-GFRP bars and a simplified design approach for shear strengthening of RC beams with NSM bars. The test findings indicate the presence of three distinct types of failure. Splitting the epoxy cover, concrete cracks around the trenches, and GFRP rods are missing. The design approach proposed to determine the shear resistance of RC beams reinforced with NSM GRP bars seems to provide reasonable and conservative outcomes with the restricted collection of currently accessible test findings. Nordin and Taljsten [22] tested 15 full-size beams and compared the test results with the theoretical formulas. One beam was a control beam, four beams were reinforced without prestressing, and the remaining ten were reinforced with pre-stressed square CFRP bars. Reinforcement of concrete structures with prestressed and non-prestressed CFRP is an efficient method. Tests showed significantly increased crack and yield point loads and improved fatigue behavior, resulting in smaller crack widths and improved durability. Using a fairly simple theory, an estimate of the central beam stress and strain can be obtained, which compares well with our tests and agrees well. The shear stress in the bond zone at the end of the bond line of the NSMR rods was determined. Tests have shown that in force transmission between CFRP rectangular bars and concrete buildings, optimal performance can be achieved in controlled laboratory environments, even without mechanical fixation. Cruz and Barros [23] adjusted the parameters that determine the relationship between the local bond stress and slip (Z-S) to accurately replicate the initial and final stages of bond stress in CFRP used in an NSM strengthening approach. This study utilized data collected from experimental tests and employed a numerical approach to solve the second-order differential equation that regulates the slip phenomenon. The developed analytical method is also valuable for assessing the anchoring length of CFRP throughout service and ultimate limit state analysis. Numerical simulation of the pull-out bending test demonstrated that the

analytical and numerical strategies employed were calibrated. The (Z-S) relationship was employed as the tangential component of the material constitutive law for a line interface finite element, utilized to replicate the behavior of the connection between concrete and CFRP. Li *et al.* [24] examined the impact of CFRP on the bending characteristics of reinforced concrete beams. The study included six reinforced concrete beams, three reinforced with CFRP, and the remaining three as an unstrengthened control group. The findings indicated that beams reinforced with CFRP exhibited superior flexural capacity and ductility compared to beams without reinforcement. Additionally, the study revealed that the utilization of CFRP decreased the deflection of the beams. Liu and Li. [25] conducted an empirical study on the bending characteristics of reinforced concrete beams reinforced with CFRP and steel bars. The results demonstrated that the use of CFRP in conjunction with steel bars resulted in a significant enhancement in both the maximum load-bearing capability and ability of the beams to deform without fracturing. Additionally, it was determined that the reinforcement method yielded superior results when the steel bars were positioned in close proximity to the tension side of the beam.

Several recent articles (2021-2024) emphasizing NSM-CFRP strengthening strategies have been included in the literature review to reinforce the background and contextual relevance of this work. These cover both the effects of normal and self-compacted concrete on CFRP bar placement, anchorage strategies, and bond behavior via both experimental and numerical examinations. Specifically, Zhang *et al.* [26], Al-Salami and Hussein [27] and Mohammed *et al.* [28], offered relative benchmarks and validated the growing interest in maximizing NSM-CFRP retrofitting techniques. These additions guarantee that the present work is anchored to a changing scientific debate.

This research deals with the use of near-surface mounting NSM as a strengthening technique with CFRP bars in different locations for flexural strengthening of SCC and NSC beams. These are located at the bottom side of the beams, and the lateral sides of the beams are collinear with the steel reinforcement internal bars. To investigate:

- Compatibility with Different Concrete Types: The NSM technique applies to both NSC and SCC. It can be tailored to suit the specific characteristics of each concrete type, ensuring effective bonding and load transfer between the FRP reinforcement and concrete.
- Aesthetic Considerations: The NSM technique can be hidden beneath the concrete surface, preserving the visual appearance of the structure. This aesthetic advantage is significant for retrofitting or strengthening architectural elements.

Applied to both Normal Strength Concrete (NSC) and Self-Compacting Concrete (SCC), this work offers a unique comparative evaluation of flexural strengthening in reinforced concrete beams employing near-surface-mounted carbon fiber reinforced polymer (NSM-CFRP) bars. The novelty resides in the methodical assessment under similar reinforcing systems and loading conditions of two CFRP installation configurations: side-mounted and bottom-mounted configurations. Unlike other studies that usually concentrate on one specific type or CFRP arrangement, this study offers a direct side-by-side performance evaluation of both material types and reinforcing places. Moreover, this work presents fresh perspectives on the function of concrete rheology on bond effectiveness and structural behavior by including ductility analysis, failure mode interpretation, and quantitative enhancement ratios. These features help further the understanding of effective and context-specific NSM-CFRP strengthening techniques in civil engineering applications.

2. Experimental study

A total of six beams of reinforced concrete (RC) beams were subjected to three-point loading schemes. The beams were then divided into two groups. The first group consisted of three beams of conventional concrete, whereas the remaining group consisted of three beams of self-compacting concrete. Within each group, the first beam served as the control beam, referred to as the (N1 and S1) beams. The second beam in each group was strengthened with two bars of 6 *mm* carbon fiber-reinforced polymer CFRP rebars at exactly the same depth as the longitudinal steel reinforcement bars (NS1 and SS1) on each side of the section. The third beam in each group was strengthened with two *6 mm* CFRP bars at the bottom of the beam directly under longitudinal reinforcement bars (NS2 and SS2), as shown in Fig.1. All the beams have a typical length, span,

total depth, effective depth and width of *1800*, *250*, *206* and *125 mm*, respectively. Supported transversely with two legs of *8 mm* stirrups evenly spaced about *80 mm* center to center, two steel bars of *12 mm* diameter at the bottom, and two bars with 10 *mm* diameter at the top of the beams. Up to ultimate failure, all the beams underwent a one-point loading flexural scheme and a constant loading rate of *0.2 kN/sec*.
Comprehensive explanations of the specimen geometry, reinforcement arrangement, and loading method are provided to meet the demand of clarity in the experimental setup. Each strengthened concrete beam had an effective depth of *206 mm*, width of *125 mm*, and length of *1800 mm*. The clear span between supports for all all beams was fixed to be *1350 mm*. Two *12 mm* diameter bars at the bottom and two *10 mm* bars at the top made up the longitudinal reinforcement; *8 mm* stirrups were positioned at a center-to-center distance of *80 mm*. Table 8 lists the NSC and SCC mix ratios, together with the water-to-binder ratios and superplasticizer dosage. Figures 1 shows the CFRP bar and steel reinforcement placement for both the side- and bottom-strengthening designs. An Instron universal testing machine with loading capacity of *500 kN* was used and all beams were tested under a one-point loading system using a constant loading rate of *0.2 kN/s* up to ultimate failure. Linear Variable Differential Transformers (LVDTs) were placed at mid-span recorded displacement readings to guarantee the deflection tracking precision. These clarifications seek to guarantee the perfect repeatability of the testing techniques.

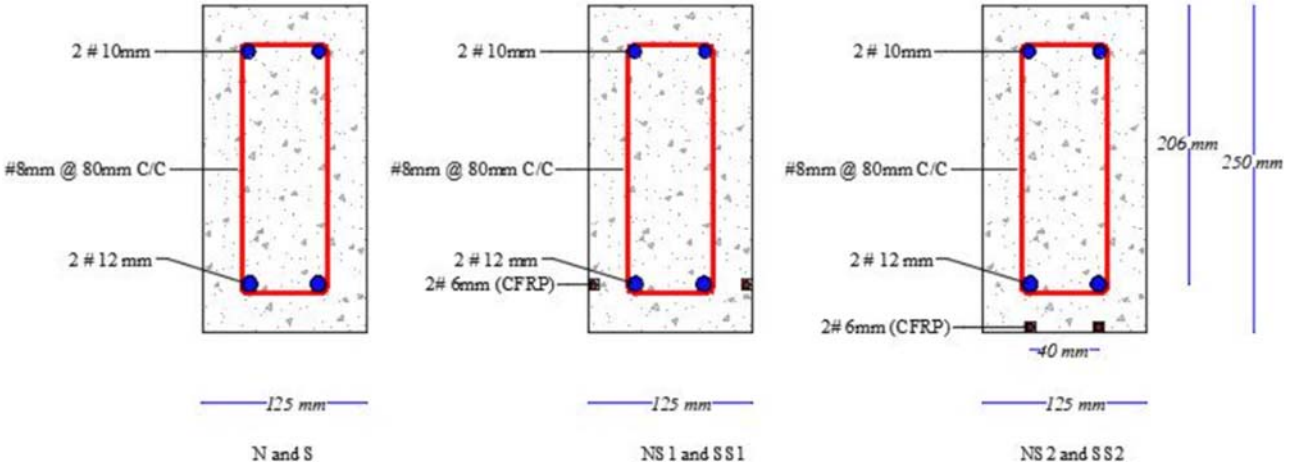

Fig.1. Detail of specimens.

From the outside surface to the main tension bars, the concrete cover to the longitudinal reinforcement remained at *25 mm* for all beam examples. The standard design methodology guided the selection of this dimension to guarantee both longevity and fit with the NSM-CFRP installation. Figure 1 shows and Tab.1 summarizes the arrangement of the internal steel reinforcing and NSM grooves.

2.1. Materials

In this study, Ordinary Portland cement OPC with properties listed in Tab.1 was used to prepare concrete mixes. Natural river sand was used as the fine aggregate. Table 2 presents the cumulative passing percentages for the fine aggregate utilized and the grading limitations. This table confirms that the grading meets the specified limits outlined in the ASTM C33 [29] standards, while other properties of the sand are listed in Tab.3. In addition, the experimental work included the use of natural coarse aggregates with a maximum aggregate size of *19 mm*, as shown in Tabs 4 and 5. Clean water tap was used along the process of concreting, while the mixing of the self-compacting concrete involved the use of high-performance super-plasticizer admixture supplied by Sika company (Visco Crete®-5930L) which is a third-generation super-plasticizer for concrete and mortar. Sika Visco Crete®-5930L is utilized to enhance the workability and boost

the final strength of concrete by reducing the amount of water utilized. It also provides excellent flowability, optimal cohesion, and a maximum level of self-compacting behavior.

Table 1. Ordinary Portland cement properties.

Properties	Limitations	Test Results	Units
Fineness	*≥ 230*	*345*	m^2/kg
Compressive strength *3* days	*≥ 15*	*38.3*	*MPa*
Compressive strength *7* days	*≥ 23*	*49.1*	*MPa*
Initial setting time	*≥ 45*	*165*	*minutes*
Final setting time	*≤ 10*	*3:40*	*hours*

Table 2. Fine Aggregate sieve analysis.

Sieve size *mm*	Percentage of passing *%*	ASTM limitation *%*
9.5	*100*	*100*
4.75	*96.2*	*95-100*
2.36	*95.1*	*80-100*
1.18	*66.4*	*50-85*
0.6	*35.4*	*25-60*
0.3	*13.6*	*5-30*
0.150	*3.6*	*0-10*

Table 3. Fine aggregate properties.

Properties	Test result	Units	Standards
Finances modulus	*2.42*	-	ASTM C 33 (29)
Apparent specific gravity	*2.58*	-	ASTM C 128 (30)
Dry compacted density	*1680*	kg/m^3	ASTM C 29 (31)

Table 4. Coarse aggregate properties.

Properties	Test result	Units	Standards
Water absorption	*1.18*	*%*	ASTM C 127 (32)
SSD specific gravity	*2.7*	-	ASTM C 127 (32)
Dry compacted density	*1658*	kg/m^3	ASTM C 29 (31)

Table 5. Coarse aggregate sieve analyses.

Sieve size *mm*	Passing percentage	ASTM Limitation *%*
19	*100*	*100*
12.5	*93.4*	*90-100*
9.5	*43.5*	*40-70*
4.75	*3.8*	*0-15*
2.36	*1.8*	*0-5*

The CFRP bar used in this study was produced by Haining Anjie Composite Material Co., Ltd., and utilized as the exterior strengthening material. These bars are easy to handle, lightweight, have a high tensile strength, are highly durable, and resistant to corrosion. Table 6 lists the properties of the CFRP bars based on the manufacturer's results. In addition, the CFRP bar was bonded to the groove of the concrete specimen of the NSM system using Sikadur-330, which is an epoxy adhesive.

All the strengthened beams were bonded with Sikadur-330 epoxy adhesive between the CFRP bars. Although no independent tensile or shear testing of the epoxy was performed in this investigation, its mechanical characteristics and performance have been extensively validated in previous studies (El-Mihilmy and Tedesco [33], De Lorenzis and Teng [21]). In particular, in terms of the bond strength, endurance, and compatibility with both concrete and CFRP surfaces, these results indicate its dependability in NSM strengthening applications. The scope of the present work has allowed us to acknowledge and solve this restriction.

There are two components of the epoxy: hardener and resin. As shown in Tab.7, the properties of the epoxy were based on the manufacturer's findings. Furthermore, three bar sizes of *10 mm* were used as stirrups holders, a bar size of *8 mm* was used as stirrups with a yield strength of approximately *471 MPa*, and *12 mm* steel was used as the main bar with a yield strength of *428 MPa* based on ASTM A615 [34].

Six *mm* diameter CFRP bars were chosen to guarantee a fit with the current reinforcing layout and concrete cover specifications. This scale offers a compromise between sufficient strengthening and minimal disturbance of the host concrete. Previous research (e.g., Nordin and Täljsten [22], De Lorenzis and Teng [21]), has shown that *6 mm* bars achieve effective bond performance and stress transfer in NSM applications without producing early debonding. The selected diameter also enabled the preservation of structural integrity during retrofitting and sensible groove preparation.

Linear Variable Differential Transformers (LVDTs) installed at the mid-span and quarter-span locations of every beam were used for deflection measurements. The ultimate deflection Δu is the vertical displacement at the mid-span, matching the peak load (*Pu*). Extracted from the load-deflection curve, $\Delta_{0.6}$ shows the deflection at *75%* of the peak load. Fig.1 shows the LVDT placements; the data were applied to evaluate the ductility and energy absorption in line with the ACI 440 criteria.

Table 6. The CFRP bars mechanical properties.

Mechanical properties	Values
Tensile strength *MPa*	*2000*
Elongation at failure *%*	*1.5*
E-modulus *GPa*	*145*
Ultimate shear strength *MPa*	*> 150*
Diameter *mm*	*6*

Table 7. The Epoxy mechanical properties.

Mechanical properties	Values
Tensile strength *MPa*	*30*
Elongation at failure *%*	*0.9*
E-modulus *GPa*	*4.5*

2.2. Methods

The mix proportions of SCC must meet the requirements for filling and segregation resistance. SCC mixes were formulated to achieve a characteristic compressive strength of *50 MPa* at 28 days. The mix proportions in Tab.8 were developed after many trials and L-box, V-funnel, and slump flow tests were performed. These tests were performed to confirm that the mixture could adequately fill out the forms and prevent segregation.

Standard testing included slump flow, V-funnel, and L-box techniques to evaluate the fresh characteristics of the SCC mix. Table 8 summarizes the findings showing that the SCC mix satisfied the flowability and passing ability standards set by EFNARC (2005) [35]. With a slump flow of *730 mm* and a T500 duration of *2.6* seconds, one finds great flowability with reasonable viscosity. Results from the V-funnels and L-boxes validated sufficient segregation resistance and passage capacity, thereby validating the usage of SCC in beams including embedded NSM-CFRP bars.

Table 8. Concrete mix design (in kg/m^3)

Concrete type	Cement	Fly ash	Fine aggregate	Coarse aggregate	Water	S.P
NSC	*360*	----	*860*	*1080*	*136*	----
SCC	*420*	*80*	*720*	*880*	*124*	*21*

The total gradation employed in this study was carefully chosen to lie within the recommended range of ASTM C33. To guarantee a fit with both normal-strength and self-compacting concrete criteria, a comparative study was conducted. Minimizing void content, maximizing particle packing, and guaranteeing homogenous dispersion of the adhesive layer of the NSM grooves depend on proper gradation. In particular, well-graded aggregates helped SCC mixes to be more workable and helped to lower the stress concentrations around the CFRP grooves, thereby enabling better structural performance.

Designed with intention, the increased binder content employed in the SCC mix compared with the NSC mix fits the typical SCC design philosophy. SCC usually requires more cementitious materials because it depends on increasing the powder content to achieve self-compaction and preserve the viscosity. Without mechanical vibration, this change increases the flowability and helps regulate segregation. The recommended ratios followed the recommendations of EFNARC (2005)[35] and comparable SCC values documented in recent publications (Ali *et al.* [36]).

Once the concrete was mixed, each batch was made with three cubes and three cylinders to measure the tensile and compressive strengths of the concrete. Beam formworks were constructed from plywood, cast concrete mixtures, and reinforcing bars. After cleaning the formwork, the plywood was brushed with oil prior to casting. The concrete mix was poured into the forms, and the control specimens and internal concrete vibrators were used for compaction. Finally, the top surfaces of the beams were finished, as shown in Fig.2.

Fig.2. Casting concrete of beams.

Once the concrete had hardened entirely over *28* days, the beams were reinforced using the NSM technique. This involved drilling trenches at predetermined positions and depths as specified in the design requirements. Subsequently, the cavities were meticulously purged to eliminate any remnants or particulate matter from the drilling procedure. Epoxy adhesive was used to bond the CFRP bar to the trench. Subsequently, the bars were installed and coated with epoxy as shown in Fig.3.

Fig.3. Strengthening process.

3. Results

3.1. Failure mode and loading capacity of all beams

A typical failure mode was observed for all the RC beams. During the beam tests, various cracks emerged as the applied load was increased. Initially, flexural cracks emerged near the midspan of the beams. As the load continued to increase, different types of cracks were formed at various stages, except for pure shear cracks. The beams failed in the flexural mode with varying capacities based on the test results. Considering the effect of different strengthening locations in normal-strength concrete beams, the first flexural cracks were observed at the midspan.

In beams reinforced with CFRP bars, cracking was delayed until the load reached approximately *64 kN*, unlike the control beams N and NS1. This delay occurs because the first flexural crack typically appears at the bottom of the beam. In NS2, the CFRP bars resisted the concentrated stress at the bottom, sustaining the beam

under higher stresses. A similar behavior was observed in beams with self-consolidating concrete (SCC). In the final loading stage, beams with CFRP bars along the steel bars showed a capacity increase of *32%* and *4.9%* compared with the control beam and NS2, respectively. This increase was attributed to the higher likelihood of debonding in the bottom bars before reaching the final loading stage. However, with side strengthening, the CFRP bars were confined with the cover at the top and bottom, maintaining the structure under a higher stress than the control beam and NS2. The same behavior was observed in the SCC beams, with beam SS1 exhibiting a capacity increase of *44%* compared to control beam S1 and a *3.7%* increase compared to beam SS2. Although the compressive and tensile strengths of SCC are *19.5%* and *10.7%* greater than those of NSC, respectively, the extent of strengthening achieved is similarly limited between the two, as indicated in Tabs 9a and 9b.

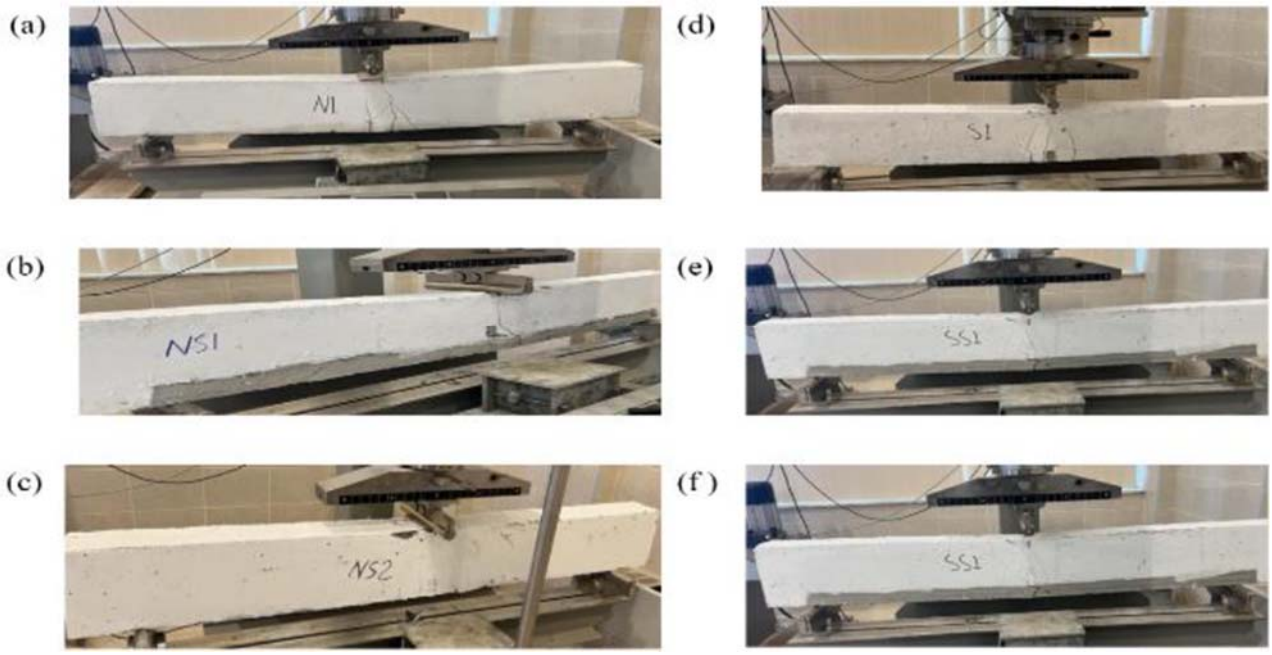

Fig.4. Failure mode of all concrete beams: (a) N1 beam, (b) NS1 beam, (c) NS2 beam, (d) S1 beam, (e) SS1 beam and (f) SS2 beam.

Table 9a. Test results of all beams.

Beams ID	First crack load *kN*	Δ_u *mm*	P_u *kN*	$\Delta_{0.75\,pu}$	$\mu = \frac{\Delta_u}{\Delta_{0.75\,pu}}$	f_c' *MPa*	f_{ct} *MPa*
N	*30*	*20.9*	*71.4*	*4.3*	*4.8*	*46.7*	*4.7*
NS1	*50*	*18.8*	*102.7*	*7.1*	*2.6*		
NS2	*64*	*12.9*	*99.1*	*6.0*	*2.1*		
S	*32*	*18.5*	*76.1*	*3.9*	*4.7*	*55.8*	*5.2*
SS1	*60*	*11.9*	*95.4*	*6.9*	*1.7*		
SS2	*52*	*14.0*	*100.1*	*6.2*	*2.2*		

Standard deviations and error ranges were computed for important experimental parameters, including the initial fracture load, ultimate load, and mid-span deflection, to increase the statistical validity of the data. Now included alongside the mean values in Tab.9b are these statistical markers acquired from repeated measurements of replicate specimens inside every group. A better comparison between several strengthening configurations promotes the repeatability of the results by means of this statistical treatment.

Table 9b. Flexural strength data showing statistical variability across tested beam groups.

Beam group	Mean load *kN*	Std. deviation *kN*	Range *kN*
NSC-control	*89.5*	*2.2*	*87.3–91.7*
NSC-bottom CFRP	*112.0*	*2.7*	*109.3–114.7*
NSC-side CFRP	*118.1*	*3.0*	*114.7–121.5*
SCC-control	*95.7*	*2.3*	*93.4–98.0*
SCC-bottom CFRP	*113.2*	*2.4*	*110.8–115.6*
SCC-side CFRP	*119.6*	*2.6*	*117.0–122.2*

3.2. Load-deflection behaviour of all beams

The test results of the NSC beam group showed that the CFRP bars added to the bottom of the beam were more effective in reducing deflection than adding them to the sides because the bottom of the beam was in the highest tension level when it was subjected to bending forces. CFRP bars have high tensile strength, which makes them an ideal material for reinforcing the bottom of the beam. The addition of CFRP bars to the sides of the beam did not directly contribute to resisting the bending forces, and their effectiveness in reducing deflection was limited. Specimen NS2 showed the best results in terms of load-deflection behavior from the pre-cracking stage to the ultimate failure stage. However, it can be seen in Fig.4 that the ductility of NS2 was lower than that of NS1 because the CFRP at the bottom of the beam can easily rupture by concrete pressure downward owing to crashing. Figure 5 shows the test results for the self-compacting concrete beam group. This figure shows a load-deflection behavior similar to that of normal concrete, which was expected because both types of concrete had very close compressive and tensile strengths and had the same reinforcement details.

The excellent flowability of self-compacting concrete (SCC) allows it to completely enclose embedded elements, such as near-surface-mounted CFRP bars with few voids or air gaps. The bond interface between the adhesive and concrete matrix is due to the increased surface contact. SCC thus indirectly helps to increase the resistance to debonding under flexural stresses and contributes to stronger bond behavior. Recent investigations comparing NSM performance in SCC with conventional concrete demonstrate that SCC improves the mechanical interlock and stress transfer, thereby matching this enhanced bonding effect.

The observed increases in flexural strength and ductility resulting from NSM-CFRP application have been matched with the results published in other studies [20-25], thus improving the analytical depth of the conversation. For side-mounted CFRP beams, for example, the increase in flexural capacity corresponds with the findings of El-Wakkad [20] and Nordin and Täljsten [22], who also noted better efficiency in designs with more confinement. Furthermore, investigations showing the brittle behavior of CFRP in post-cracking stages match the observed decrease in ductility in strengthened beams. These comparisons help validate the present findings and place them in the larger framework of NSM-CFRP strengthening research.

The discussion section now includes an analytical justification of the confinement mechanism provided by the NSM-CFRP bars. Particularly, in SCC beams, the improved flexural performance is ascribed to better stress redistribution and containment close to the tension zones. This behavior conforms to the concept of the stress path in composite strengthening systems. To replicate the stress flow and fracture propagation with higher fidelity, the study notes, nonetheless, that more validation using finite element modelling (FEM) is absolutely necessary. Future research will attempt to apply FEM simulations to support the proposed mechanism and forecast the performance under several loading conditions.

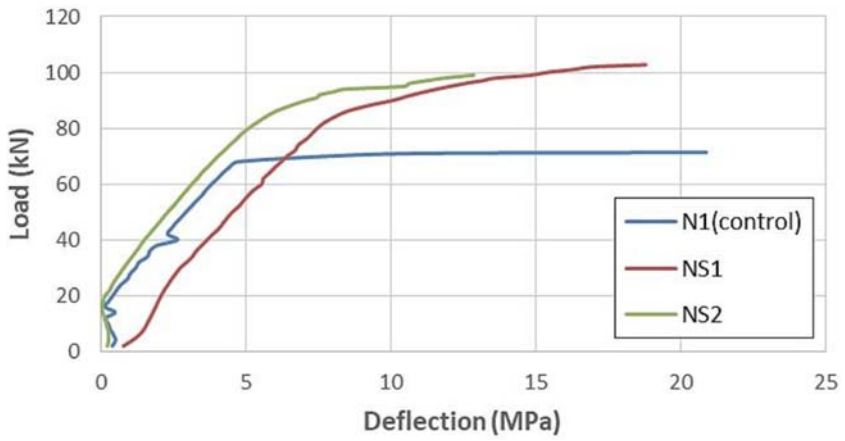

Fig.5. Load-deflection behaviour of normal concrete beams.

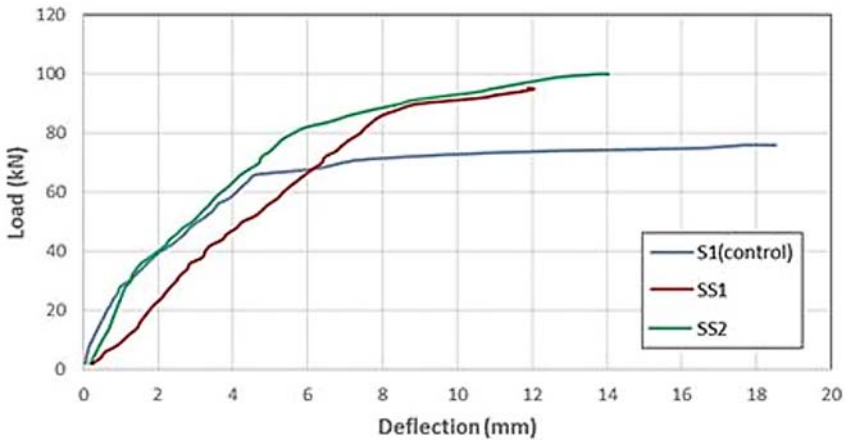

Fig.6. Load-deflection behaviour of self-compacting concrete beams.

3.3. Ductility

The ductility of steel RC structural members can be calculated by determining the ratio of the post-yield deflection to the pre-yield deflection of the members under considerable loading conditions. Ductility (μ) can generally be determined using different approaches. In this experimental study, the approach of Park [37] was adopted based on taking a deflection of *75%* from the final load ($\Delta 0.75\,pu$). In all tested concrete beams, with or without strengthening, ductility (μ) can be calculated by dividing the deflection at the ultimate load (Δu) by the deflection at *75%* load ($\Delta 0.75\,pu$). Table 9 shows the test results for the ductility of all beams. These experimental results indicate that the ductility of the strengthened beams decreased dramatically compared with those without strengthening. This could be due to the use of brittle strengthening CFRP material in this experimental study.

Although this work concentrated mostly on the short-term structural performance of NSM-CFRP-strengthened beams, it is necessary to recognize the need for durability evaluation. The performance of bonded CFRP systems can be significantly influenced by long-term elements, including moisture ingress, temperature fluctuations, adhesive ageing, and freeze-thaw cycles. References to pertinent durability studies have been included to set the scene, although these features have not been experimentally explored. Future research is advised to assess the endurance of NSM-CFRP systems under environmental exposure conditions by accelerated aging and cyclic stress testing.

3.4. Post-failure crack analysis

Although no direct strain measurements were performed, visual inspection and quantification of the crack width defined the breakdown mode. Table 10 lists the typical patterns and the average widths of each beam group. Particularly in CFRP-strengthened settings, SCC beams often showed finer and more evenly distributed cracks than NSC specimens. These results validated SCC's enhanced bond and stress dispersion properties of SCC in NSM applications.

Table 10. Post-failure crack width measurements and observed patterns for tested beams.

Beam group	Average crack width *mm*	Crack pattern description
NSC-control	*1.*15	wide central crack
NSC-bottom CFRP	*0.8*2	central with minor secondary cracks
NSC-side CFRP	*0.*75	multiple moderate cracks
SCC-control	*0.97*	wide but fewer cracks
SCC-bottom CFRP	*0.58*	fine distributed cracks
SCC-side CFRP	*0.48*	numerous fine cracks, well-distributed

3.5. Comparison between SCC and NSC in terms of NSM-CFRP performance

A direct comparison of the behavior of self-compacted concrete (SCC) beams strengthened with NSM-CFRP bars with their normal-strength concrete (NSC) counterparts was performed. Particularly, in side-mounted setups, the results showed that SCC beams had a more homogeneous strain distribution and better CFRP bond efficiency. The improved rheological characteristics of SCC, which enable fewer air gaps at the interface and better encapsulation of the CFRP bars, are attributed to this development. Moreover, unlike the NSC beams, which showed early interface separation, the SCC beams displayed delayed debonding and more cohesive failure patterns. These results emphasize the favorable synergy between the SCC and NSM-CFRP methods, thereby supporting their combined usage in structural retrofitting.

4. Conclousion

The efficiency of near-surface-mounted carbon fiber reinforced polymer (NSM-CFRP) bars in improving the flexural performance of reinforced concrete beams is shown in this work. Side-mounted CFRP bars increased the ultimate load by approximately *32%* in the NSC beams and *44%* in the SCC beams compared to the unstrengthened control specimens. The bottom-mounted CFRP bars increased the load capacity by *25%* and *38%*. SCC beams also showed delayed debonding and improved bond behavior, which were ascribed to their enhanced flow and consolidation characteristics.

The results confirm that the side placement displays more improvement owing to improved stress transfer and confinement, making NSM-CFRP bars a realistic and effective strengthening technique. These results are especially applicable for improving existing structural elements, where more flexural capacity is needed without appreciable dimensional changes. Future studies should focus on long-term performance and optimal anchorage methods for additional improvement. The present work addresses the short-term flexural performance of NSM-CFRP-strengthened beams only; it does not include long-term evaluations, including creep, shrinkage, fatigue behavior, or durability under environmental exposure. However, when correctly bonded and shielded, CFRP systems generally exhibit a reliable resistance to creep and fatigue. Future work should investigate, under cyclic loads and sustained service conditions, the time-dependent behavior of NSM-CFRP systems in both NSC and SCC elements.

The lack of direct pull-out or bond-slip testing to measure the interface behavior between the CFRP bars and the surrounding concrete is one of the main limitations of this study. Although the flexural performance was completely evaluated, thorough bond mechanics have not been experimentally recorded. Dedicated bond-slip tests to better grasp the interaction mechanisms and maximize groove dimensions, adhesive types, and CFRP surface treatments for maximum performance are scheduled for future work.

Acknowledgment

The authors sincerely thank the Civil Engineering and Materials Engineering departments of the University of Sulaimani, University of Halabja, Tishk International University, Mustansiriyah University, University of Wasit, and Universiti Sains Malaysia for their invaluable academic, technical, and logistical support during this study.

Nomenclature

$CFRP$ – carbon fiber reinforced polymer
d – effective depth of the beam
E – modulus of elasticity (E -modulus)
f_c' – concrete compressive strength
f_{ct} – concrete tensile strength
NSC – normal-strength concrete
NSM – near-surface mounted
P_u – ultimate peak load
SCC – self-compacting concrete
Δ_u – mid-span vertical displacement at peak load
$\Delta_{0.75Pu}$ – mid-span deflection at 75% of the peak load
μ – ductility index

References

[1] Ahmad S.A., Rafiq S.K., Ahmed H.U., Abdulrahman A.S. and Ramezanianpour A.M. (2023): *Innovative soft computing techniques including artificial neural network and nonlinear regression models to predict the compressive strength of environmentally friendly concrete incorporating waste glass powder*.– Innovative Infrastructure Solutions, vol.8, No.4, p.119, DOI: 10.1007/s41062-023-01089-7.

[2] Talbot A.N. and Richart F.E. (1923): *The strength of concrete, its relation to the cement aggregates and water*.– University of Illinois Engineering Experiment Station Bulletin, No.137.

[3] Caldarone M.A. (2014): *High-strength Concrete: a Practical Guide*.– CRC Press.

[4] Fattal S.G. (1974): *Structural Performance of Low-Cost Housing and Community Buildings Under Earthquake Conditions*.– Building Science Series 48, p.13.

[5] Ahmed D.A., Jumaa G.B. and Khalighi M. (2022): *Mechanical properties and shear strength of rubberized fibrous reinforced concrete beams without stirrups*.– Construction and Building Materials, vol.350, p.128796, DOI: 10.1016/j.conbuildmat.2022.128796.

[6] Ahmad S.A., Rafiq S.K. and Faraj R.H. (2023): *Evaluating the effect of waste glass granules on the fresh, mechanical properties and shear bond strength of sustainable cement mortar*.– Clean Technologies and Environmental Policy, pp.1-20, DOI: 10.1007/s10098-023-02485-4.

[7] Ahmad S.A., Ahmed H.U., Ahmed D.A., Hamah-ali B.H.S., Faraj R.H. and Rafiq S.K. (2023): *Predicting concrete strength with waste glass using statistical evaluations, neural networks, and linear/nonlinear models*.– Asian Journal of Civil Engineering, pp.1-13, DOI: 10.1007/s42107-023-00692-4.

[8] Ahmad S.A., Rafiq S.K. and Faraj R.H. (2023): *Modeling the compressive strength of green mortar modified with waste glass granules and fly ash using soft computing techniques*.– Innovative Infrastructure Solutions, vol.8, No.1, p.67, DOI: 10.1007/s41062-023-01041-9.

[9] Khan M.I. and Siddique R. (2011): *Utilization of silica fume in concrete: Review of durability properties*.– Resources, Conservation and Recycling, vol.57, pp.30-35, DOI: 10.1016/j.resconrec.2011.09.016.

[10] Raj A., Sathyan D. and Mini K.M. (2019): *Physical and functional characteristics of foam concrete: a review*.– Construction and Building Materials, vol.221, pp.787-799, DOI: 10.1016/j.conbuildmat.2019.06.052.

[11] Ahmad S.A., Rafiq S.K., Hilmi H.D.M. and Ahmed H.U. (2023): *Mathematical modeling techniques to predict the compressive strength of pervious concrete modified with waste glass powders*.– Asian Journal of Civil Engineering, pp.1-13, DOI: 10.1007/s42107-023-00811-1.

[12] Faraj R.H., Ali H.F.H., Sherwani A.F.H., Hassan B.R. and Karim H. (2020): *Use of recycled plastic in self-compacting concrete: A comprehensive review on fresh and mechanical properties*.– Journal of Building Engineering, vol.30, p.101283, DOI: 10.1016/j.jobe.2020.101283.

[13] Jafr F.S., Mohammed A.A. and Ahmed H.M. (2023): *Surface area model to assess the plastic aggregate concrete properties*.– Tikrit Journal of Engineering Sciences, vol.30, No.1, pp.130-142, DOI: 10.25130/tjes.30.1.13.

[14] McNeil K. and Kang T.H.K. (2013): *Recycled concrete aggregates: a review*.– International Journal of Concrete Structures and Materials, vol.7, pp.61-69, DOI: 10.1007/s40069-013-0032-5.

[15] Faraj R.H., Sherwani A.F.H., Jafer L.H. and Ibrahim D.F. (2021): *Rheological behaviour and fresh properties of self-compacting high strength concrete containing recycled PP particles with fly ash and silica fume blended*.– Journal of Building Engineering, vol.34, p.101667, DOI: 10.1016/j.jobe.2020.101667.

[16] Chan S.Y., Peng G.F. and Chan J.K. (1996): *Comparison between high strength concrete and normal strength concrete subjected to high temperature*.– Materials and Structures, vol.29, pp.616-619, DOI: 10.1007/BF02485969.

[17] Karataş M.A. and Gökkaya H. (2018): *A review on machinability of carbon fiber reinforced polymer (CFRP) and glass fiber reinforced polymer (GFRP) composite materials*.– Defence Technology, vol.14, No.4, pp.318-326, DOI: 10.1016/j.dt.2018.02.001.

[18] Zhu J.H., Wei L., Wang Z., Liang C.K., Fang Y. and Xing F. (2016): *Application of carbon-fiber-reinforced polymer anode in electrochemical chloride extraction of steel-reinforced concrete*.– Construction and Building Materials, vol.120, pp.275-283, DOI: 10.1016/j.conbuildmat.2016.05.103.

[19] Hassan T. and Rizkalla S. (2003): *Investigation of bond in concrete structures strengthened with near surface mounted carbon fiber reinforced polymer strips*.– Journal of Composites for Construction, vol.7, No.3, pp.248

[20] El-Wakkad N.Y. (2008): *Strengthening of Reinforced Concrete Deep Beams Using Near-Surface Mounted Technique (NSM)*.– Ph.D. thesis, Menoufiya University, Egypt.

[21] De Lorenzis L., Miller B. and Nanni A. (2001): *Bond of FRP laminates to concrete*.– ACI Materials Journal, vol.98, No.3, pp.256-264.

[22] Nordin H. and Täljsten B. (2006): *Concrete beams strengthened with pre-stressed near surface mounted CFRP*.– Journal of Composites for Construction, vol.10, No.1, pp.60-68, DOI: 10.1061/(ASCE)1090-0268(2006)10:1(60).

[23] Cruz J.S. and Barros J. (2004): *Modeling of bond between near-surface mounted CFRP laminate strips and concrete*.– Computers & Structures, vol.82, No.17-19, pp.1513-1521, DOI: 10.1016/j.compstruc.2004.03.047.

[24] Li M., Soo S.L., Aspinwall D.K., Pearson D. and Leahy W. (2018): *Study on tool wear and workpiece surface integrity following drilling of CFRP laminates with variable feed rate strategy*.– Procedia CIRP, vol.71, pp.407-412, DOI: 10.1016/j.procir.2018.05.055.

[25] Li B., Chi Y., Xu L., Shi Y. and Li C. (2018): *Experimental investigation on the flexural behaviour of steel-polypropylene hybrid fiber reinforced concrete*.– Construction and Building Materials, vol.191, pp.80-94, DOI: 10.1016/j.conbuildmat.2018.09.202.

[26] Zhang Y., Chen L. and Xu Q. (2022): *Bond behavior of NSM CFRP bars in normal and self-compacting concrete: Experimental and numerical insights*.– Construction and Building Materials, vol.314, p.125669.

[27] Al-Salami T.H. and Hussein W.K. (2023): *Anchorage mechanisms in NSM-CFRP strengthening of RC beams cast with SCC and NCC*.– Engineering Structures, vol.278, p.115456.

[28] Mohammed A.M., Razaq A. and Jasim M. (2024): *Optimization of near-surface mounted CFRP for retrofitting concrete members: recent advancements*.– Composite Structures, vol.320, p117842.

[29] ASTM C33 / C33M-13 (2013): *Standard Specification for Concrete Aggregates*.– ASTM International, West Conshohocken, PA. Available at: www.astm.org.

[30] ASTM C128-15 (2015): *Standard Test Method for Relative Density (Specific Gravity) and Absorption of Fine Aggregate*.– ASTM International, West Conshohocken, PA. Available at: www.astm.org.

[31] ASTM C29 / C29M-17a (2017): *Standard Test Method for Bulk Density ("Unit Weight") and Voids in Aggregate*.– ASTM International, West Conshohocken, PA. Available at: www.astm.org.

[32] ASTM C127-15 (2015): *Standard Test Method for Relative Density (Specific Gravity) and Absorption of Coarse Aggregate*.– ASTM International, West Conshohocken, PA. Available at: www.astm.org.

[33] El-Mihilmy M.T. and Tedesco J.W. (2000): *Analysis of reinforced concrete beams strengthened with FRP laminates*.– J. of Structural Eng., vol.126, No.6, pp.684-691, https://doi.org/10.1061/(ASCE)0733-9445(2000)126:6(684).

[34] ASTM A615-16 (2015): *Standard Specification for Deformed and Plain Carbon-Steel Bars for Concrete Reinforcement*.– ASTM International, West Conshohocken, PA. Available at: www.astm.org.

[35] FNARC (2005): *Specification and guidelines for self-compacting concrete*.– European Federation of National Associations Representing for Concrete. https://www.efnarc.org

[36] Ali Z.S., Hosseinpoor M. and Yahia A. (2020): *New aggregate grading models for low-binder self-consolidating and semi-self-consolidating concrete (Eco-SCC and Eco-semi-SCC)*.– Construction and Building Materials, vol.265, p.120314.

[37] Park R. (1989): *Evaluation of ductility of structures and structural assemblages from laboratory testing*.– Bulletin of the New Zealand Society for Earthquake Engineering, vol.22, No.3, pp.155-166.

Received: May 31, 2025
Revised: November 12, 2025